Chapter X
Spring Pendulum

X.1 A Brief Introduction

In its simplest form, the spring pendulum consists of a mass attached to a lightweight vertical rod held in position by a spiral spring. Clearly the pendulum is inverted, and the system is actually an *inverted Duffing oscillator*, the Duffing oscillator is a much-loved and well-understood system. Details of the apparatus are shown in Fig.1.

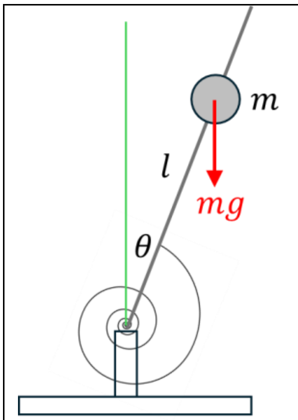

Figure 1. Vertical pendulum with spring restoring force.

The mass m can be moved to a particular distance l from the pivot point, we take l as our principal system parameter. The system will clearly perform oscillations around the vertical.

X.2 The Simple Spring Pendulum System

X.2.1 Equations of Motion

The 2nd-order ODE describing the system dynamics follows by considering angular motion around the pivot. We have, where k is the spring stiffness and $I = ml^2$ the moment of inertia of the pendulum bob

$$I\ddot{\theta} = mgl\sin\theta - k\theta \qquad (1)$$

For small θ we can expand the sin term as usual to obtain

$$\ddot{\theta} = \left(\frac{mgl - k}{I}\right)\theta - \frac{mgl}{6I}\theta^3 \qquad (2)$$

If we take θ as *very* small, i.e. $\theta \ll 1$, and for the case where $k > mgl$, (which means that the spring dominates over gravity) then we obtain the linear system

$$\ddot{\theta} = -\omega^2\theta \qquad (3)$$

which describes oscillations about the vertical with frequency

$$\omega = \sqrt{\left(\frac{k - mgl}{I}\right)} \qquad (4)$$

Then the expression for small θ becomes

$$\ddot{\theta} = -\omega^2\theta - \frac{mgl}{6I}\theta^3 \qquad (5)$$

Using the established language of the Duffing oscillator, the cubic term leads to a 'hard' spring since the period decreases with amplitude.

Eq.(5) has a single fixed point θ =0, about there are very small oscillations of frequency given by eq.(4). This solution, however, is not of particular interest in our study. Much more interesting is the case where $k < mgl$ where gravity dominates over the spring. The expression for small θ now becomes

$$\ddot{\theta} = \sigma^2\theta - \frac{mgl}{6I}\theta^3 \qquad (6)$$

where

$$\sigma = \sqrt{\left(\frac{mgl - k}{I}\right)} \qquad (7)$$

Clearly this is not a harmonic oscillator since the force due to the linear term is positive and therefore not restoring.

The behaviour of this system can be gleaned by plotting the angular acceleration $\ddot{\theta}$ as a function of θ. This is shown in Fig.2 where we have selected *m* = 1 and *k* = 4.905 as our standard parameters.

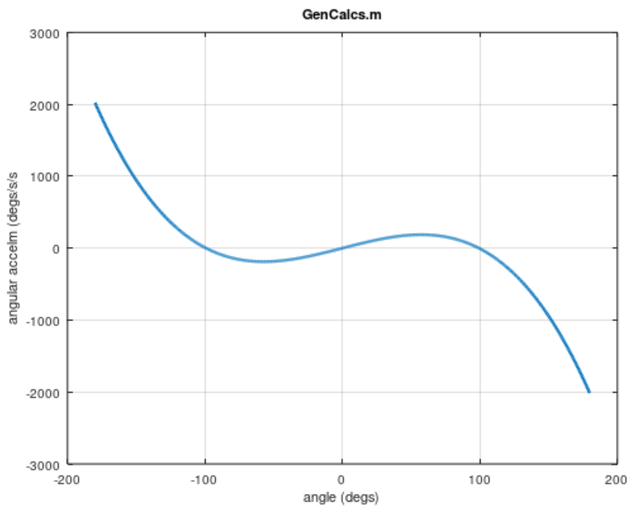

Figure 2. Angular acceleration as a function of angle. There are three equilibrium values, one unstable (angle is zero) and two stable (angle plus and minus about 100 degrees).

There are three fixed points, an unstable equilibrium at $\theta = 0$ and two stable equilibria. From eq.6 we find these are at

$$\theta_{equ} = \pm\sqrt{\frac{6I}{mgl}\sigma} \qquad (8)$$

This means that the bob is never stable in a vertical position but must lean to one side or the other.

Finally, we can use eq.2 to obtain an expression for θ_{equ} as a function of the physical parameters, *m*, *g*, *l*, and *k*.

$$\theta_{equ} = \pm\sqrt{6\left(1 - \frac{k}{mgl}\right)} \qquad (9)$$

This is an important expression since it tells us that we can *choose* either *k*, *m*, *g*, or *l* as our principal parameter for studies (independent variable or bifurcation parameter). Our choice is further guided by looking at the numerator in eq.(4) and eq.(7) which can be zero. We choose *l* as our principal parameter, and therefore identify a 'critical length' for our system,

$$l_c = k/mg \qquad (10)$$

which indicates how the linear components of spring and gravity are balanced. We can then write eq.(9) as

$$\theta_{equ} = \pm\sqrt{6\left(1 - \frac{l_c}{l}\right)} \qquad (11)$$

where the necessary condition $l > l_c$ for this solution type corresponds to our original condition $k > mgl$.

Also we can choose to rewrite eq.(7) as

$$\sigma = \sqrt{\frac{g}{l}}\sqrt{\left(1 - \frac{l_c}{l}\right)} \qquad (12)$$

Both of these equations clearly reflect critical behaviour at $l = l_c$; we shall use these to plan our investigations.

X.2.2 Frequencies of Oscillation

For small amplitude oscillations these may be obtained using the gradient of the acceleration. Around a stable fixed point we have look for oscillations of frequency ω so that

$$\ddot{\theta} = -\omega^2\theta \qquad (13)$$

but in approximation we have

$$\ddot{\theta} = -\left.\frac{d\ddot{\theta}}{d\theta}\right|_{equi}\Delta\theta \qquad (14)$$

and since

$$\left.\frac{d\ddot{\theta}}{d\theta}\right|_{equi} = -2\sigma^2 \qquad (15)$$

we expect the local oscillations to have frequency

$$\omega = \sqrt{2}\sigma \qquad (16)$$

X.2.3 Experimental Results

Here we report the results of various simulation studies and compare to the theory developed above, especially eq.(11) for the equilibrium angles and eq.(12) for the oscillation frequency at each angle. Fig.3 shows the pitchfork bifurcation with branches to the right of l_c given by eq.(11) shown as a solid curve with experimental data as circles for parameters m = 1, k = 4.905 with

$l_c = 0.5$. (Here m and k were chosen to give the stated critical length).

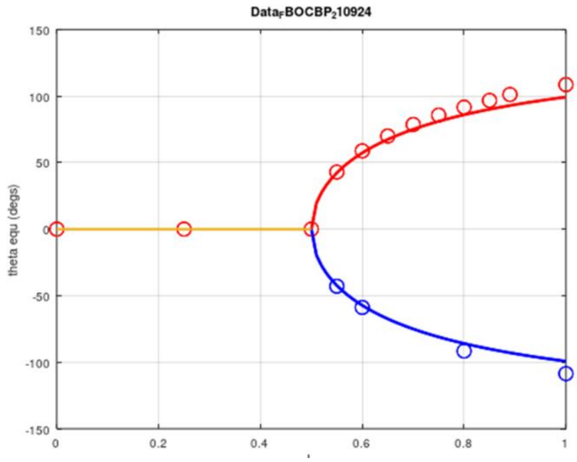

Figure 3.Plot of equilibrium angle as a function of pendulum length *l*. The pendulum can be found with equal chance on each side of the vertical. Lines are from eq.(11), circles show simulation results.

The variation of period with length *l* is shown in Fig.4 where solid lines are the theoretical solutions using eq.(4) below the critical point and eq.(16) above. The large increase of period close to the critical point (rising to infinity at that point) is clearly visible.

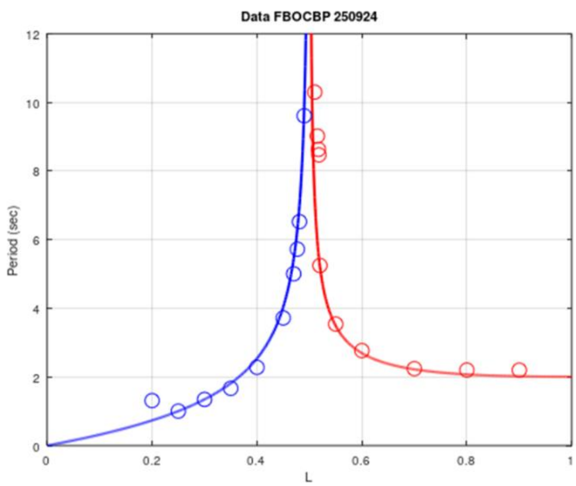

Figure 4. Variation of period with length both above and below the critical length of 0.5. Lines are solutions of eq.(4) and eq.(16) with circles showing simulation results.

X.3 The Tilted Spring Pendulum

X.3.1 Equations of Motion

The symmetry of the simple spring pendulum may be broken by arranging the base of the system to be tilted at an angle α as shown in Fig.5. Note that θ is measured from the vertical. We can easily imagine some possible solutions: With $\alpha > 0$ the pendulum will prefer to move clockwise and so might find an equilibrium there, but it might not, if the length l is small or the spring is very stiff. So it is perhaps not so easy to imagine *realistic* solutions, so we must resort to analysis.

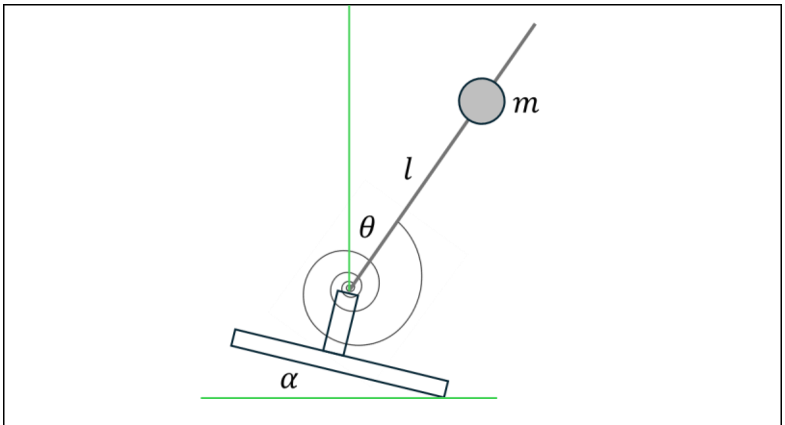

Figure 5. Pendulum titled from the vertical by angle α.

Before we delve into the analysis, let’s consider on investigation for a value of $\alpha = 1^o$. The resulting bifurcation curve is shown in Fig.6; data points are shown as circles and the solid lines are interpolations through the points.

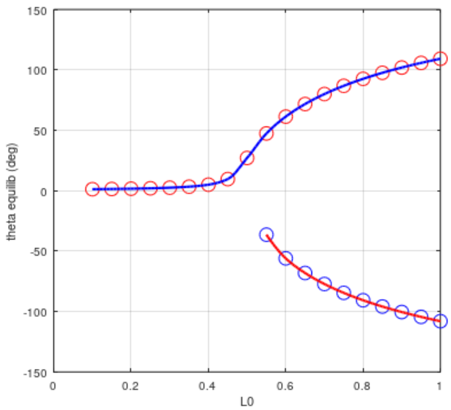

Figure 6. Simulated data points for equilibrium angle as a function of pendulum length (circles) with interpolated lines.

This can be usefully compared with Fig.3, here we see the symmetry of the curve has been broken. When we actually perform an experiment, we start with $L = 1$, obtain the equilibrium value of θ, then reduce L. Starting on the top branch (with the pendulum located clockwise) we proceed smoothly to construct the upper branch. But starting on the bottom branch (with the pendulum located anticlockwise) something interesting happens; when we are at about $L = 0.55$ and reduce the length even further, the pendulum suddenly jumps over to the right, back onto the top branch. There is a range of L where no negative-θ solutions are possible.

We must now lay down the theory to understand this. The equation of motion becomes

$$I\ddot{\theta} = mgl\sin\theta - k(\theta - \alpha) \qquad (17)$$

where for the case of small θ we obtain the following expression which should be compared to eq.(6)

$$\ddot{\theta} = \sigma^2\theta - \frac{mgl}{6I}\theta^3 - \frac{\alpha k}{I} \qquad (18)$$

X.3.2 The Solution Surface

Stationary solutions of this expression are obtained by setting $\ddot{\theta} = 0$ which leads to the following, after a little cleaning up,

$$\alpha + \left(\frac{l}{l_c} - 1\right)\theta - \frac{l}{l_c}\frac{\theta^3}{6} = 0 \qquad (19)$$

This is an *implicit* equation for θ and defines a *surface* where $\theta = f(\alpha, l_c)$ which can be plotted numerically in Fig.7 where we have used $\beta = l/l_c$.

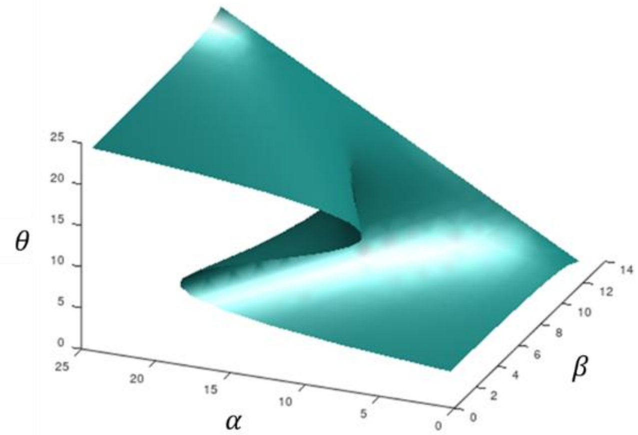

Figure 7 Solution surface for equ.(19) where the equilibrium angle is a function of $\alpha$and β.

This surface contains all possible solution for the pendulum angle θ as a function of the system parameters α and $\beta = L/L_c$. It's the latter parameter which is our principal or bifurcation parameter.

The key feature of this surface is that it contains a *fold* and when this is projected onto the $\alpha - \beta$ plane we obtain a *cusp* which delineates several regions where the solution is different. Perhaps the easiest way to understand the range of solutions is to plot the associated potential wells at some (α, β) points, see Fig.8.

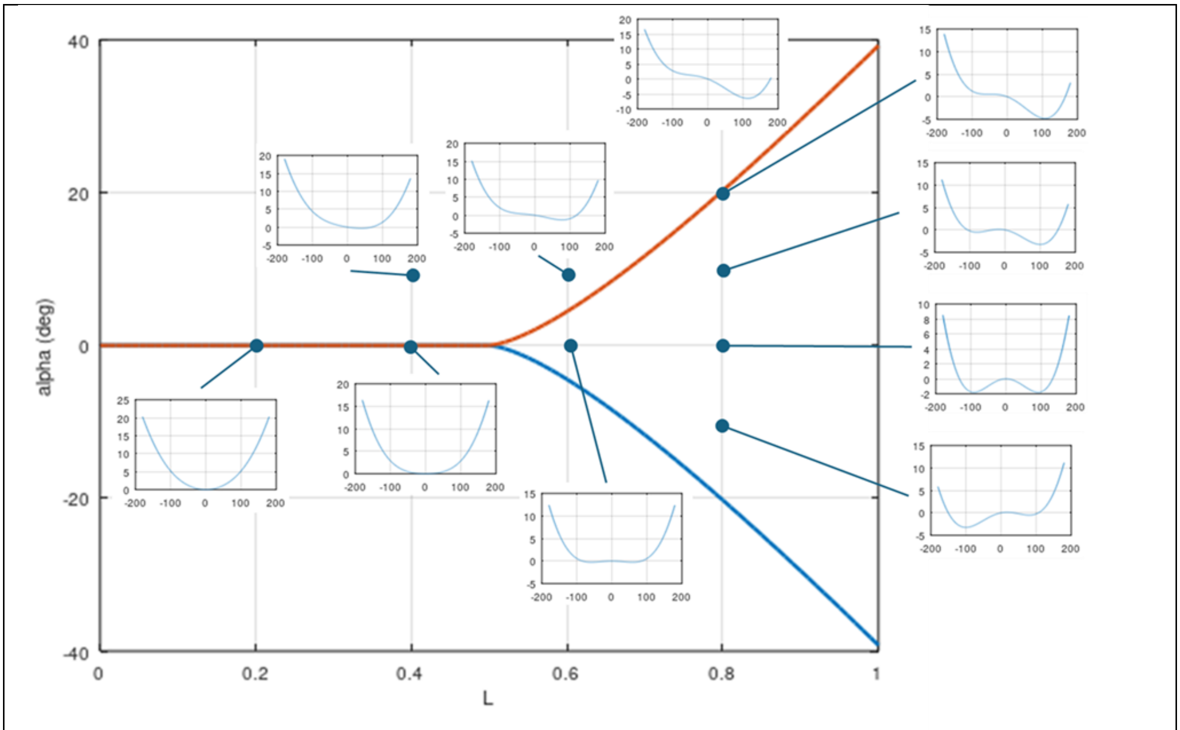

Figure 8. Potential wells for some selected values of length *l* and parameter

Let's first consider the solutions where $\alpha = 0$ increasing β from zero. All potential wells are symmetrical, which must be the case since the platform is not tilted. To the left of the cusp we have a single well centred on 0, so we will have oscillations about this point. Then, as we move to the right of the cusp, the well bifurcates and we have two minima. So we expect two solutions, oscillations with the same frequency but about different equilibrium points. As β is increased, the location of these points moves further from the origin.

Now consider keeping β fixed at $\beta = 0.8$ and let α increase from -30 to 30. We see the relative depths of the two potential wells changes, for negative tilt α the negative well is deeper, so there is more chance of finding the oscillator here. As we move through $\alpha = 0$ then the rightmost well becomes deeper, and we expect to find the oscillator with a positive angle. Finally as we leave the cusp, there is only one well, the rightmost. So oscillations must be around a positive angle.

X.3.3 Jumps in the System Solution

Let's return to the 3D surface and ask ourselves what it means to increase α while keeping β constant. Hopefully Fig.9 will help clarify the meaning of the jump. The idea is that we go on a journey and move along a path on the lower surface as shown by the red arrow.

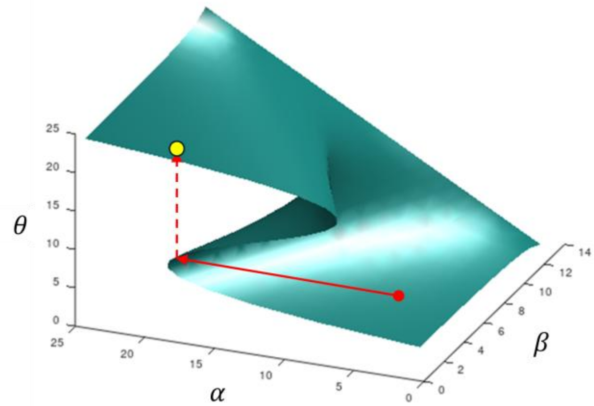

Figure 9. Journey along the solution surface starting at the red dot and moving to the left. At a certain point you run out of lower surface and have to jump to the upper part of the surface.

We move smoothly along the bottom surface and pass through the lower cusp; we see that the equilibrium value of θ also smoothly changes, steadily increasing. But then we hit the *fold* in the surface. What happens, where do we go? The only place is to make a jump up to the top surface and we end up at the yellow circle. This *jump* implies a sudden change in the solution, θ has suddenly, discontinuously, jumped to a large value.

Returning to our cusp diagram, this trajectory has moved through all the solutions within the cusp (for $\beta = 0.8$) but none of these solutions are actually realized. The results of an experiment making just this path are shown in Fig.10. The blue curve shows the angle of the oscillator as the value of α was increase manually starting at -30 degrees, these values are shown in red. A small amount of system damping was added to allow a *smooth* path across the solution surface.

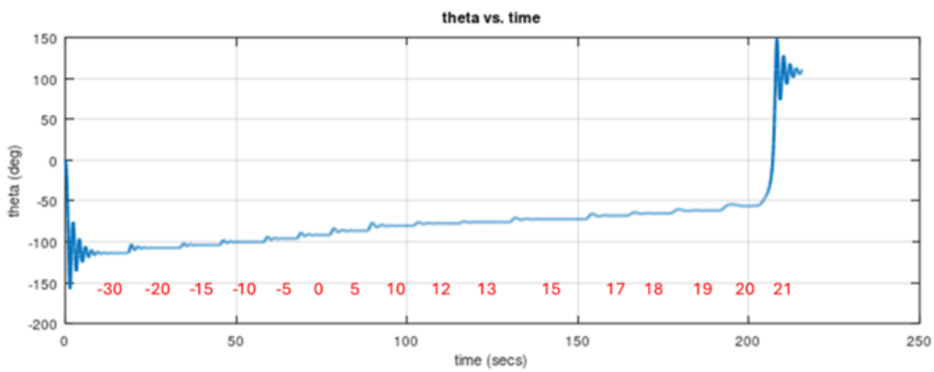

Figure 10. Simulation investigation starting at a negative α (red numbers) and slowly increasing α. At the critical point, the solution jumps to the higher branch.

The solution changes smoothly as we traverse the cusp (-20 to +20 degrees) but jumps when we leave the cusp (20 degrees).

X.3.4 The Solution Surface and the Bifurcation Curve

We must now relate the bifurcation curve (see Fig.6) which is defined by the solution angle as a function of β for constant α. This is clearly a projection of the solution onto the $\beta - \theta$ plane located by α.

A slice through the surface for a small range of α is shown in Fig.11 which clearly reproduces the shape of the bifurcation curve, Fig.6 above.

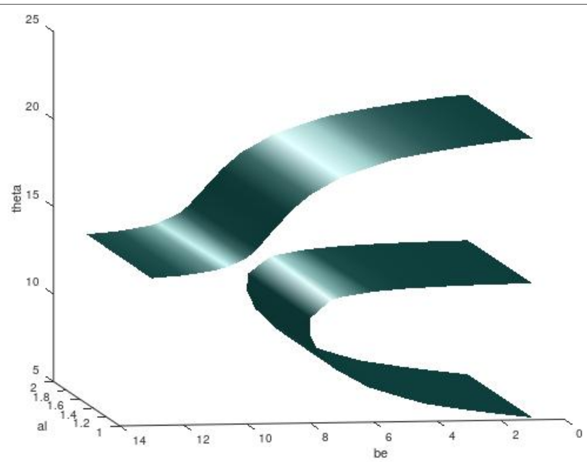

Figure 11. Slice through the solution surface showing the bifurcation curve.

X.3.5 Some Experimental Results

It is useful to compare two sets of experimental results, one for $\alpha = 1^o$ and the other for $\alpha = 10^o$ corresponding to a small and a larger platform tilt. The results are shown in Fig.12. Solid curves are the theoretical solutions, the blue is calculated from eq.(19) which is an approximation, the red are exact solutions computed implicitly from the equilibrium condition without approximation

$$l = \frac{l_c}{\sin\theta}(\theta - \alpha) \qquad (20)$$

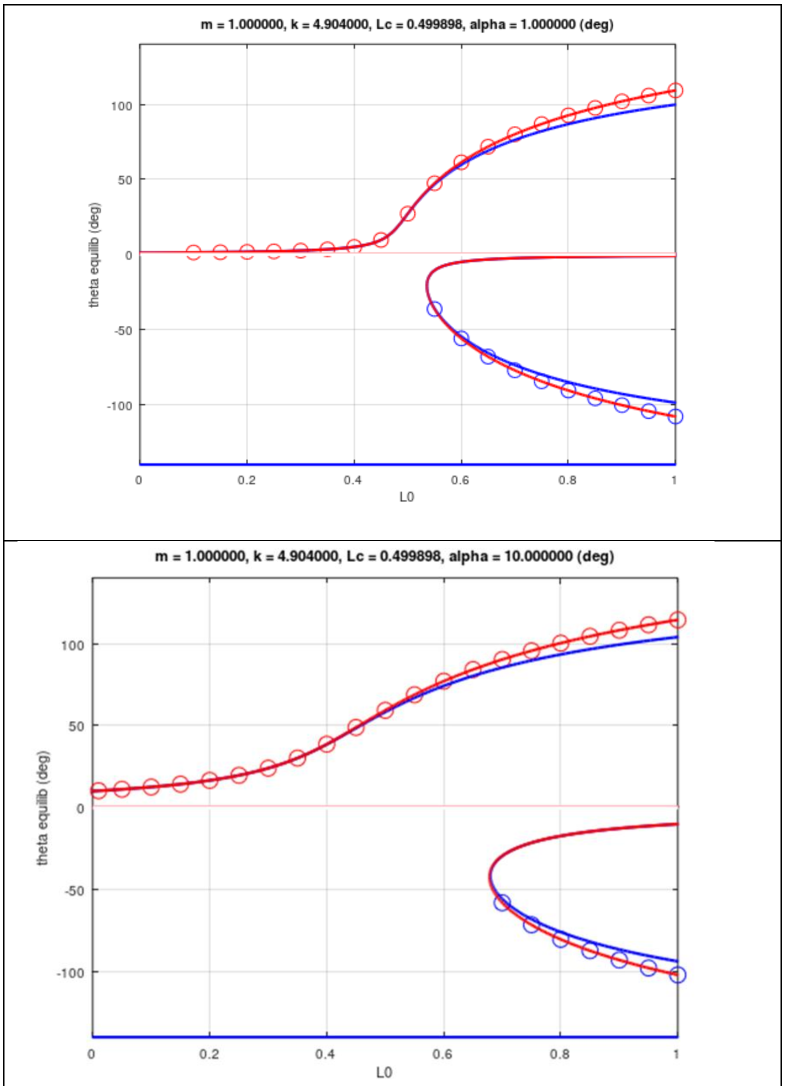

Figure 12. Bifurcation curves for two values of α: Top $\alpha = 1$deg, bottom $\alpha = 10$deg.

There is a clear difference in the bifurcation unfolding; for $\alpha = 10^o$ there is a larger gap between the upper and lower branch stable solutions. This is hardly surprising since a larger tilt implies a larger propensity for deflection in the direction of the tilt. Looking at the lower branch, where $\theta < 0$ we see that a larger pendulum length is required to obtain stable solutions. Again this is not surprising since a larger anticlockwise torque is needed to offset the spring torque due to the clockwise tilted platform. Looking at the upper branch, for $\alpha = 10^o$ the variation with L is much smoother, again because here the pendulum has propensity to deflect in the tilt direction.

X.3.6 Study of Frequency Dependency